

XMM-Newton imaging of V1818 Ori: a young stellar group on the eastern edge of the Kappa Ori ring. [★]

I. Pillitteri¹, S. J. Wolk², and S. T. Megeath³

¹ INAF-Osservatorio Astronomico di Palermo, Piazza del Parlamento 1, 90134 Palermo, Italy
e-mail: pilli@astropa.inaf.it

² Harvard-Smithsonian Center for Astrophysics, 60 Garden St, Cambridge (MA), 02138 USA

³ Ritter Astrophysical Research Center, Dept. of Physics and Astronomy, University of Toledo, Toledo, OH, USA

Received; accepted

ABSTRACT

We present the results of a 40 ks *XMM-Newton* observation centered on the variable star V1818 Ori. Using a combination of the *XMM-Newton* and *AllWISE* catalog data, we identify a group of about 31 young stellar objects around V1818 Ori. This group is coincident with the eastern edge of the dust ring surrounding κ Ori. Previously, we concluded that the young stellar objects on the western side of ring were formed in an episode of star formation that started 3–5 Myr ago, and are at a distance similar to that of kappa Ori (250 – 280 pc) and in the foreground to the Orion A cloud. Here we use the *XMM-Newton* observation to calculate X-ray fluxes and luminosities of the young stars around V1818 Ori. We find that their X-ray luminosity function (XLF), calculated for a distance of ~ 270 pc, matches the XLF of the YSOs west of κ Ori. We rule out that this group of young stars is associated to Mon R2 as assumed in the literature, but rather they are part of the same κ Ori's ring stellar population.

Key words. stars: formation — stars: individual(V1818 Ori, Kappa Ori) — stars: activity

1. Introduction

Understanding the spatial structure and distribution of young stellar objects (YSOs) in the Orion molecular cloud complex is crucial for tracing its star formation history. The Orion OB association is characterized by several subgroups of stars of different masses, ages and distances; its southern portion, Orion A, has distances between ~ 388 pc and 428 pc (Kounkel et al. 2017; Bally 2008; Menten et al. 2007). The Orion region thus offers a wide spectrum of test cases for various mechanisms of star formation, e.g., self collapse vs. triggered star formation, interplay of external agents as opposed to in situ evolution, or formation of low mass groups in isolation vs. mass segregated formation in denser and more massive clusters.

In this context, we investigated the X-ray emission of YSOs west of κ Ori and to the South of Orion A/L1641 Pillitteri et al. (2016). These young stars are within a ring of gas and dust apparently surrounding the B0 (V) star κ Ori within a radius of 2 deg (Fig. 1). The ring appears as the rim of a bubble created by the sweeping action of the stellar winds emanating from κ Ori. This structure overlaps the L1641 region of the Orion A cloud. However, the quoted distance to κ Ori is about $200 - 240 \pm 40$ pc (Megier et al. 2009; van Leeuwen 2007), much closer than Orion A (around 400 pc). We thus investigated the relationship between the YSOs in the ring and Orion A. By means of X-ray observations of the YSOs in the ring of dust and the comparison of their X-ray luminosity function to that of L1641 and ONC stars, we determined that the distance to the YSOs near κ Ori is about 250 – 280 pc, similar to the κ Ori distance, and as such

they are unrelated to Orion A. They are rather a distinct population of YSOs born within the ring of gas and dust centered on κ Ori visible in extinction maps and mid IR and sub-mm images.

V1818 Ori is a Herbig Be star surrounded by about two dozen of YSOs and apparently sitting on the eastern edge of the same ring of dust centered on κ Ori (Fig. 1). V1818 Ori has highly irregular variability and bursts (Chiang et al. 2015), and it is a binary system with components separated by $3.5''$. The spectra show strong veiling perhaps due to active accretion, and the stellar variability could also affect the determination of its spectral type, which is B7 as reported by Chiang et al. (2015) but it is F0 as classified by Connelley & Greene (2010). Based on the similarity of velocity of the stellar absorption lines with that of the gas towards the Mon R2 association, Chiang et al. (2015) assumed that these YSOs are part of the Mon R2 star forming complex at a distance of 900 pc. However, given its coincidence with the κ Ori' ring, the issue of the distance to V1818 Ori remains unsolved.

In the present paper we analyze an *XMM-Newton* observation centered on V1818 Ori to resolve the issue of the distance to V1818 Ori and its nearby YSOs, to search for evidence of young stars to the east of κ Ori and to establish the extent and spatial structuring of the ongoing star formation in the ring.

The paper is structured as following: in Sect. 2 we present the observation and the data analysis, in Sect. 3 we present our results and we discuss them, in Sect. 4 we present our conclusions.

2. Observation and data analysis

We observed the region towards V1818 Ori with *XMM-Newton* on April 6 2017 for a nominal duration of 40 ks (PI: Ignazio Pil-

[★] Based on observations obtained with XMM-Newton, an ESA science mission with instruments and contributions directly funded by ESA Member States and NASA

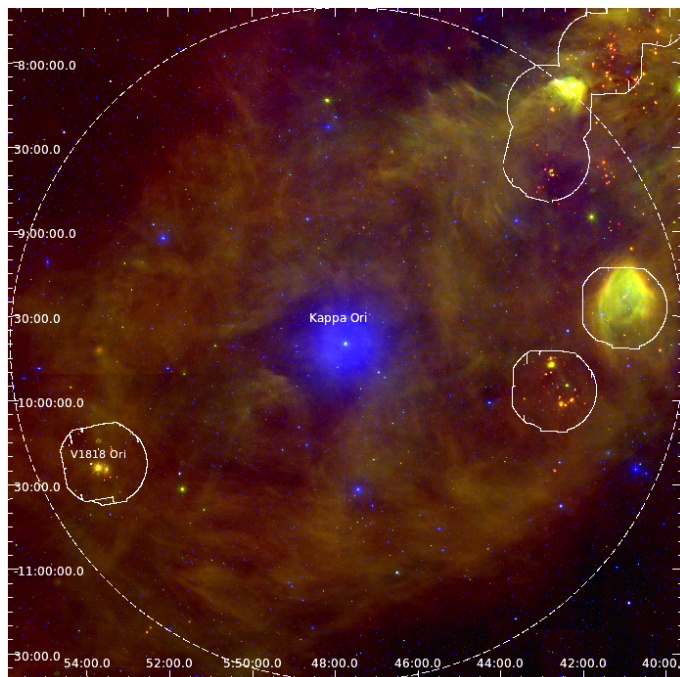


Fig. 1. Composite RGB Optical (blue) + WISE 12 μ m (green) and 22 μ m (red) centered on κ Ori. With white contours we mark on the right side the *XMM-Newton* fields observed in Pillitteri et al. (2016) and Pillitteri et al. (2013), and to the left the field around V1818 Ori. The ring of warm dust is visible in the WISE bands and extends ~ 2 deg from κ Ori (dashed large circle).

litteri, ObsId 0800190101). The nominal pointing was at R.A. = $05^h53^m30^s$, Dec. = $-10^d22^m30.8^s$ (J2000) about 3 arcmin offset from the optical position of V1818 Ori. We used EPIC as a prime instrument and the *Medium* filter. Figure 2 shows a composite RGB image of the *XMM-Newton* observation in three bands: 0.3-1.0 keV (red), 1.0-3.0 keV (green), and 3.0-8.0 keV (blue).

We used SAS ver. 15 to reduce the data and obtain tables of events calibrated in astrometry, energy and timing. We selected the events of MOS 1, MOS 2 and *pn* in the 0.3-8.0 keV band, with FLAG = 0 and PATTERN ≤ 12 as prescribed by the SAS guide.

The background was highly variable during the observation and, in order to maximize the signal to noise of faint sources, we used the light curve at high energies ($E > 10$ keV) and a cut in rate to select good time intervals and filter out intervals with high background. At this step we removed about 15 ks leaving thus 25 ks of low background exposure, this is the portion of exposure time that we used for the subsequent source detection process. The source detection was made with a wavelet convolution technique implemented in a FORTRAN code that finds local maxima in the wavelet convolved image at different wavelet scales (Damiani et al. 1997a,b). We used a threshold of 4.6σ of local background to identify local maxima as X-ray sources, this value should retain, at most, one spurious source in the image due to statistical fluctuations of the background. We detected 91 point-like sources; we can also recognize by eye a couple of faint extended sources to the north east corner of the image that have two radio galaxies as likely counterparts.

We searched for infrared counterparts to the X-ray sources in the *AllWISE* catalog (Wright et al. 2010; Cutri & et al. 2014) using a matching radius of $5''$, and identified 50 X-rays sources with 50 WISE objects. We supplement these with the remaining WISE point sources within the *XMM-Newton* field of view (Fig

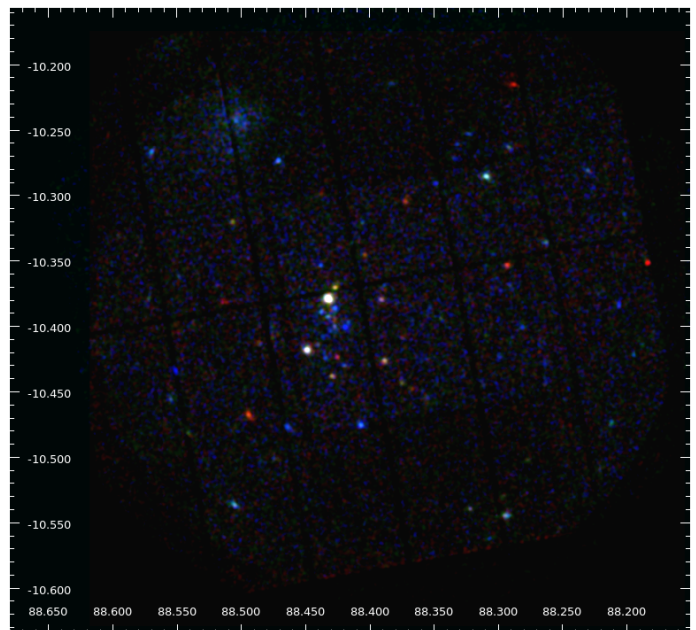


Fig. 2. Composite RGB image of V1818 Ori as observed with *XMM-Newton*. The color bands are: 0.3-1.0 keV (red), 1.0-2.5 keV (green), and 2.5-5.0 keV (blue). About 91 point like sources and two faint extended sources are detected in the image.

3). The WISE mid-IR color-color and color-magnitude diagrams show sources with distinct IR excesses: $W2 - W3 > 1.1$ mag and $W1 - W2 > 0.3$ mag. We selected the sources with $W2 \leq 12$ mag as YSOs; fainter sources are likely to be extragalactic (Koenig et al. 2012; Koenig & Leisawitz 2014). Two objects with $W1 - W2 > 1.5$ mag are identified as protostars; the remainder as stars with disks (Class II; Koenig et al. 2012, Fischer et al. 2016). We further identify sources with $W2 - W3 > 1.5$ mag, $W2 \leq 12$ mag, and $W1 - W2 < 0.3$ mag as transition disks. X-ray sources with $W2 - W3 < 1.1$ mag and $W2 \leq 12$ mag were classified as disk-less pre-main sequence stars (Class III objects). Another 12 objects with X-ray emission have near-IR colors and magnitudes similar to young pre-main sequence stars, i.e., no detections in $W3$ and $W4$ bands, and $W1 - W2$ colors less than 0.3 mag (Fig 3); these are classified as Class III objects. Finally, we required $J - Ks > 0.47$ for sources detected in these bands; this eliminated one Class III source with a color bluer than that expected for pre-main stars (Fig. 3). The *AllWISE* images were visually inspected as for the quality flags, signal to noise estimates, and χ^2 values of the selected YSOs. Two X-ray sources that satisfy the criteria for transition disks are affected by artifacts from V1818 Ori; these are reclassified as Class III objects. Four additional X-ray sources are found with $W2$ between 13.6 and 14.6 mag, $W2 - W3 < 2$ mag (using upper limits in the $W3$ band), and J -band magnitudes fainter than 14.8 mag. We exclude these from our catalog for two reasons. First, these stars show J -band magnitudes below the Hydrogen burning limit for 3 Myr pre-main sequence stars at distance up to 400 pc (Baraffe et al. 1998). Second, the spatial position of such objects are more spread than the group of YSOs surrounding V1818 Ori, thus as a conservative choice we excluded them. Future spectroscopic observations are needed to determine whether they are truly pre-main sequence stars. The remaining X-ray sources with IR counterparts are much fainter ≥ 16 mag and are not considered members. About 41 X-ray sources are left without IR counterparts. In Pillitteri et al. (2016) 47/238 (in two *XMM* fields) were left

without IR counterparts, i.e. about 23-24 per XMM field. Here we have almost twice the number of X-ray sources without IR matches. An inspection of the XMM image revealed that most of them have blue colors, this means their spectra are either hard or heavily absorbed. They are scattered in the XMM field of view while the YSOs are concentrated toward the center. Taken together, the spatial distribution and spectral hardness indicate a background population. The presence of a background cluster of galaxies is not excluded, the two extended sources found in the image could be part of it, although we cannot find a galaxy cluster listed in the 2MASS (Tully 2015) and SDSS catalogs (Tempel et al. 2012) within 20 arcmin from V1818 Ori.

Upper limits to rates were calculated at a threshold consistent with the value used for source detection. The conversion factor (CF) between rates and unabsorbed fluxes (0.3-8.0 keV band) was derived with PIMMS ver. 4.9. We assumed a thermal coronal spectrum described by an APEC model with $kT = 1$ keV, $Z = 0.2Z_{\odot}$. The average absorption was estimated from an extinction map¹ (Schlafly & Finkbeiner 2011), and a value of $E(B - V) \sim 1$ from which we derive $N_H = 6.3 \times 10^{21} \text{ cm}^{-2}$ (corresponding to $A_V \sim 3.3$ mag, for $R_V = 3.1$, Cardelli et al. 1989, value reported in the reddening vector in Fig. 3). With these choices the CF has a value of $2.078 \times 10^{-11} \text{ erg cm}^{-2}$. Local higher extinction and a different plasma temperature can change the CF by about 50%. Given the low count statistics of the sources and the short exposure time it is impossible to perform a more accurate spectral analysis to derive their temperatures and fluxes.

3. Results and discussion

We identified 31 members in the V1818 Group: 2 protostars (one with X-ray detection), 15 Class II sources (11 with X-ray detections), one X-ray undetected transition disk object, and 13 X-ray identified Class III sources (Table 1). Due to spatial overlap with a nearby source in the *ALLWISE* data, one of the Class II sources without an X-ray detection is considered tentative (see Table 1 notes). The disk fraction among the YSOs with a X-ray detection is 0.46 ± 0.14 . Chiang et al. (2015) identified 24 YSOs in the V1818 Ori group using a combination of WISE colors and near-IR observations with the Subaru telescope. Twelve out of 24 YSOs selected by Chiang et al. are in common with our selection of members of the V1818 Ori group. The remaining 12 YSOs are not recovered by our criteria since they have WISE magnitudes below our limits or were identified in higher angular resolution, deeper near-IR observations. Table 1 lists the 31 YSOs identified as members of the V1818 Ori group.

These 31 YSOs including V1818 Ori form a group of pre main sequence stars coincident with the eastern edge of the dust ring surrounding κ Ori.

From the fluxes listed in Table 1, we calculated luminosities and we used a Kaplan-Meier estimator (as implemented in the R package *survival* in the case of left-censored data) to assess the distribution of the X-ray luminosities (XLFs) of the V1818 Ori's group on a set of distances between 115 pc and 1000 pc and used the Kolmogorov-Smirnov (KS) test to compare with the XLF of the YSOs found on the western edge of the κ Ori' ring. This is a relative distance analysis, but having assessed the distance to the Kappa Ori's YSOs in Pillitteri et al. (2016) this analysis will be also calibrated in an absolute scale. The Kappa Ori' XLF extends up to $10^{31} \text{ erg s}^{-1}$ and is more skewed than the one of V1818 Ori. Since the number of points in the two XLFs differ by a factor of

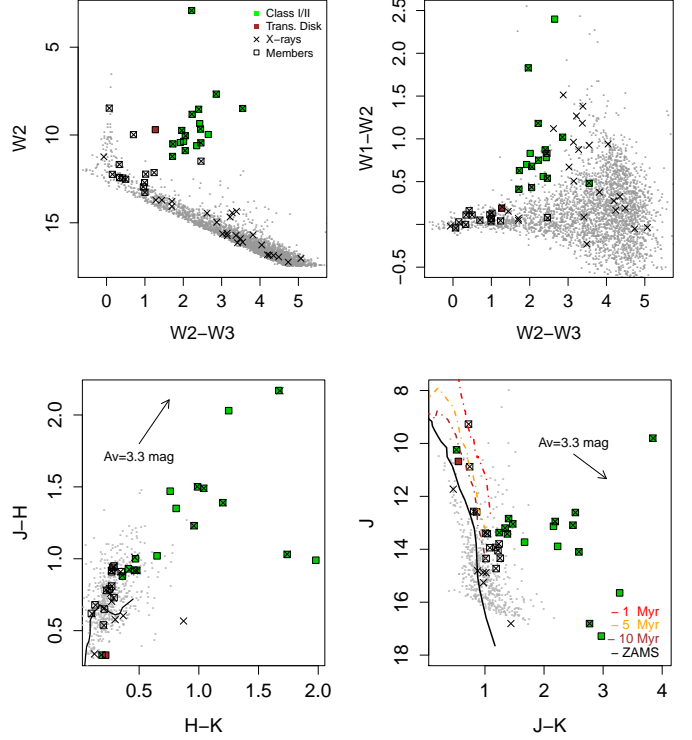


Fig. 3. Top panels: WISE color-color and color-magnitude diagrams of the objects in the *XMM-Newton* field of view. W1, W2 and W3 refer to the 3.4 μm , 4.6 μm and 12 μm WISE bands. Selected members of the V1818 Ori group are open squares. Bottom panels: 2MASS color-color and color-magnitude diagrams. Solid line represents the zero age Main Sequence, dashed lines are isochrones at 1, 5 and 10 Myr, respectively, for a distance of 270 pc (distance moduli for 270 pc, 400 pc and 900 pc are ~ 7.2 mag, ~ 8 mag and ~ 9.1 mag, respectively). The reddening vector corresponding to $A_V = 3.3$ mag represents the average extinction in the *XMM-Newton* field.

~ 8 , we can speculate that the high luminosity tail in Kappa Ori' XLF could be due to flaring sources or to few foreground objects contaminating the sample.

The KS statistic peaks at a distance of ~ 270 pc and the 90% confidence range is $\sim 230 - 350$ pc. For $d = 400$ pc the KS statistic is ~ 0.06 and for 900 pc the KS statistic is $\sim 2 \times 10^{-6}$. A distance of $d = 900$ pc appears unrealistic, thus we can safely exclude that V1818 Ori and its surrounding YSOs belong to the Mon R2 association as suggested by Chiang et al. (2015). A distance of $d = 400$ pc still appears higher than expected as the two XLFs overlap very marginally at the high luminosity tails, while $d \sim 270$ pc seems the most reasonable. V1818 Ori and the surrounding YSOs seem unrelated to Orion A and L1641 and to the Mon R2 association. Rather, they are likely part of the κ Ori ring as they form a clump inside the eastern edge of it, analogous to the groups of YSOs identified on the western edge of the ring (Pillitteri et al. 2016).

Based on the low background exposure time of 25 ks, the completeness limit is estimated above $L_X > 10^{29} \text{ erg s}^{-1}$ at a distance of 270 pc. This could leave undetected some very low mass stars. Assuming a saturated X-ray luminosity and a ratio $L_X/L_{bol} \sim 10^{-3}$, we have detected stars with $L_{bol} \geq 10^{32} \text{ erg s}^{-1}$ or about $0.1 L_{bol,\odot}$, this value corresponds to spectral types of M5, M4 and M2, respectively, when adopting isochrones at 1, 5 and 10 Myr (Siess et al. 2000). The fraction of undetected YSOs with IR excesses is about 33%, this alone suggests that the

¹ <http://irsa.ipac.caltech.edu/applications/DUST/>

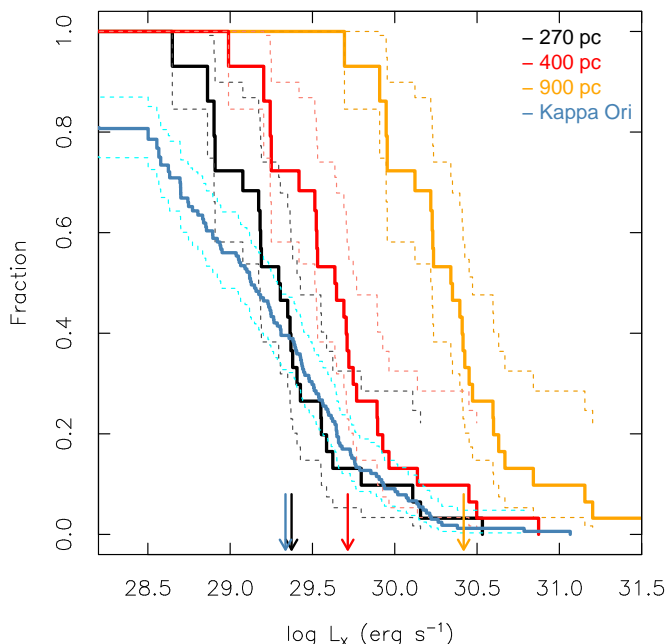


Fig. 4. Kaplan-Meier estimators of the X-ray Luminosity Function of the YSOs in V1818 Ori calculated for three distances: 900 pc (orange), 400 pc (red) and 270 pc (black). The curves at the 95% confidence range are plotted in dashed lines. The XLF of the YSOs associated with Kappa Ori (Pillitteri et al. 2016) is shown for comparison. The arrows mark the medians of the different XLFs. The best agreement to the XLF of Kappa Ori group (distance 250–280 pc) is obtained for a distance of 270 pc.

average distance of these objects is unlikely to be 900 pc as for the Mon R2 region.

The IR classification revealed only one protostar or Class I object in the *XMM-Newton* FOV. The paucity of protostars and the fraction of stars with disks suggest an age of 2 – 5 Myr, similar to that estimated for the YSOs on the western edge of the ring of κ Ori and slightly younger than the age of κ Ori itself (Pillitteri et al. 2016).

Considering the whole population of stars within 2 deg of κ Ori, its most massive member is κ Ori itself (a B0 star), then V1818 Ori is the second massive known member, followed by several low mass, M type stars. Initial results from an optical spectroscopic survey of the YSOs identified in Pillitteri et al. (2016) reveal that these are predominantly low mass, M-type objects (Pillitteri et al., in prep.). We speculate that the group of YSOs around V1818 Ori is composed mostly of M type stars as well. Including the sources from Pillitteri et al. (2016), about 152 YSOs formed in the past 2 – 5 Myrs within the κ Ori ring, resulting in a rate of star formation of 30-75 stars Myr^{-1} .

4. Conclusions

We have presented the results from the analysis of an *XMM-Newton* observation of the group of young stellar objects around the variable young star V1818 Ori, which is associated with the Mon R2 region at 900 pc. However, given that the group is coincident with the eastern edge of the ring of warm dust surrounding κ Ori at ~ 250 pc, we investigated their X-ray properties to infer their distances and ages analogously to what was done in Pillitteri et al. (2016).

About 91 point-like X-ray sources and two faint extended sources were detected in 0.3-8.0 keV band. About 50 X-ray sources have an infrared counterpart in WISE catalog. We used *AllWISE* and 2MASS photometry to identify 31 objects as members of the group, including 25 X-ray sources, and classify them as protostars, Class II, III and transition disks. We calculated the X-ray fluxes and luminosities (0.3-8.0 keV band) for the 25/31 YSOs detected in X-rays and upper limits to fluxes and luminosities for the remaining 6/31. By using a set of different distances for calculating the luminosities and comparing the resulting X-ray luminosity function (XLF) to that of the YSOs west of κ Ori, we concluded that 900 pc is unrealistic and the group of V1818 Ori is not related to Mon R2. A distance of 400 pc is still marginally consistent with the XLF of κ Ori group, and thus the group does not appear related to Orion A and L1641. For a distance of 270 pc (90% confidence interval in 230 – 350 pc) we obtain our best agreement with the XLF of the YSOs west of κ Ori and the median X-ray luminosity of COUP YSOs. We conclude that V1818 Ori and its surrounding young stars were born in the eastern edge of the κ Ori ring and are part of it.

Acknowledgements. IP acknowledges support from INAF, ASI and the ARIEL consortium. SJW was supported by NASA contract NAS8-03060 (Chandra X-ray Center). This publication makes use of data products from the Wide-field Infrared Survey Explorer (WISE) and the Two Micron All Sky Survey (2MASS) retrieved through the NASA / IPAC Infrared Science Archive.

References

- Bally, J. 2008, Overview of the Orion Complex (Reipurth, B.), 459–+
- Baraffe, I., Chabrier, G., Allard, F., & Hauschildt, P. H. 1998, A&A, 337, 403
- Cardelli, J. A., Clayton, G. C., & Mathis, J. S. 1989, ApJ, 345, 245
- Chiang, H.-F., Reipurth, B., & Hillenbrand, L. 2015, AJ, 149, 108
- Connelley, M. S. & Greene, T. P. 2010, AJ, 140, 1214
- Cutri, R. M. & et al. 2014, VizieR Online Data Catalog, 2328
- Damiani, F., Maggio, A., Micela, G., & Sciortino, S. 1997a, ApJ, 483, 350
- Damiani, F., Maggio, A., Micela, G., & Sciortino, S. 1997b, ApJ, 483, 370
- Fischer, W. J., Padgett, D. L., Stapelfeldt, K. L., & Sewilo, M. 2016, ApJ, 827, 96
- Koenig, X. P. & Leisawitz, D. T. 2014, ApJ, 791, 131
- Koenig, X. P., Leisawitz, D. T., Benford, D. J., et al. 2012, ApJ, 744, 130
- Kounkel, M., Hartmann, L., Loinard, L., et al. 2017, ApJ, 834, 142
- Megier, A., Strobel, A., Galazutdinov, G. A., & Krelowski, J. 2009, A&A, 507, 833
- Menten, K. M., Reid, M. J., Forbrich, J., & Brunthaler, A. 2007, A&A, 474, 515
- Pillitteri, I., Wolk, S. J., & Megeath, S. T. 2016, ApJ, 820, L28
- Pillitteri, I., Wolk, S. J., Megeath, S. T., et al. 2013, ApJ, 768, 99
- Schlaflly, E. & Finkbeiner, D. P. 2011, in Bulletin of the American Astronomical Society, Vol. 43, American Astronomical Society Meeting Abstracts #217, 434.42
- Siess, L., Dufour, E., & Forestini, M. 2000, A&A, 358, 593
- Tempel, E., Tago, E., & Liivamägi, L. J. 2012, A&A, 540, A106
- Tully, R. B. 2015, AJ, 149, 171
- van Leeuwen, F. 2007, A&A, 474, 653
- Wright, E. L., Eisenhardt, P. R. M., Mainzer, A. K., et al. 2010, AJ, 140, 1868

Table 1. List of identified YSOs and their 2MASS, WISE and X-ray photometry. Objects in common with Chiang et al. (2015) are indicated. Detection significance is given in units of the local background σ . Unabsorbed fluxes are given in the 0.3-8.0 keV band. For undetected YSOs the rates and fluxes are upper limits. Notes indicate contamination from spikes or bright nearby objects and names of objects known in literature.

N.	RA J2000 (deg)	Dec J2000 (deg)	designation	J	H	Ks	W1 mag	W2	W3	W4	Classification	Chiang Id	Rate ct ks ⁻¹	Error	Signif σ_{bkg}	log Flux	Note
1	88.29435	-10.5443	J055310.64-103239.6	13.9	13.0	12.8	12.5	12.4	12.1	8.08	Class III	-	7.09	0.55	20.60	-12.83	
2	88.32193	-10.5394	J055317.26-103221.8	13.4	12.5	12.1	11.6	11.2	9.5	7.67	Class II	-	1.27	0.24	9.10	-13.58	
3	88.29679	-10.5301	J055311.22-103148.2	13.8	12.8	12.6	12.4	12.2	11.2	7.89	Class III	-	1.41	0.30	5.90	-13.53	
4	88.54125	-10.4813	J055409.89-102852.7	14.1	13.1	12.8	12.6	12.4	12.0	8.72	Class III	-	2.12	0.46	8.80	-13.36	
5	88.49402	-10.4679	J055358.56-102804.3	12.6	11.9	11.8	11.7	11.7	11.3	8.64	Class III	-	3.45	0.36	14.30	-13.14	
6	88.37462	-10.4431	J055329.90-102635.1	14.7	13.8	13.5	13.3	13.3	12.3	8.93	Class III	-	0.85	0.14	8.10	-13.75	
7	88.42907	-10.4383	J055342.97-102617.9	13.0	12.0	11.6	10.7	10.0	7.99	5.84	Class II	7	1.23	0.16	12.70	-13.59	
8	88.38821	-10.4269	J055333.17-102536.8	13.4	12.6	12.4	12.2	12.1	10.9	7.82	Class III	-	1.96	0.19	17.00	-13.39	
9	88.42543	-10.4237	J055342.10-102525.3	12.6	11.9	11.7	11.6	11.5	9.03	7.59	Class III	-	0.66	0.12	7.90	-13.86	W3 Contaminated
10	88.44868	-10.4184	J055347.68-102506.1	12.8	11.9	11.4	11.0	10.4	7.99	5.62	Class II	21	7.91	0.40	41.80	-12.78	
11	88.44001	-10.4141	J055345.60-102450.7	12.9	11.7	10.8	9.4	8.53	6.13	3.62	Class II	20	0.44	0.11	5.50	-14.04	
12	88.48618	-10.4128	J055356.68-102446.1	13.4	12.6	12.4	12.3	12.2	12.1	8.99	Class III	-	0.82	0.17	6.80	-13.77	
13	88.37511	-10.4092	J055330.02-102432.9	10.2	9.91	9.72	8.97	8.49	4.94	2.84	Class II	2	0.40	0.10	4.70	-14.08	IRAS05510-1025
14	88.42729	-10.4002	J055342.54-102400.5	9.8	7.63	5.96	4.09	2.91	0.69	-1.07	Class II	1	0.45	0.10	7.40	-14.03	V1818 Ori
15	88.41904	-10.4009	J055340.97-102403.0	12.6	11.1	10.1	8.69	7.67	4.81	1.52	Class II	15	1.47	0.20	10.50	-13.51	
16	88.41640	-10.3975	J055339.93-102350.9	13.1	11.6	10.6	9.57	8.82	6.59	3.22	Class II	14	0.25	0.08	5.00	-14.29	
17	88.43755	-10.3894	J055345.01-102321.9	14.1	12.7	11.5	10.5	9.66	7.21	4.39	Class II	19	0.85	0.14	9.60	-13.76	
18	88.39081	-10.3798	J055333.79-102247.3	13.4	12.5	12.0	11.1	10.5	8.78	7.01	Class II	9	1.32	0.16	13.50	-13.56	
19	88.43200	-10.3793	J055343.68-102245.3	10.9	10.3	10.1	10	9.98	9.28	6.76	Class III	-	18.80	0.57	72.60	-12.41	W3 Contaminated
20	88.42676	-10.3708	J055342.42-102214.7	13.2	12.3	11.9	11.3	10.9	8.84	6.79	Class II	-	2.32	0.27	19.20	-13.32	
21	88.40408	-10.3455	J055336.97-102043.7	13.9	13.1	12.9	12.8	12.7	11.7	9.05	Class III	-	1.09	0.18	8.60	-13.65	
22	88.50644	-10.3202	J055401.54-101912.7	14.3	13.4	13.1	12.6	12.5	12.0	8.53	Class III	-	1.98	0.28	11.20	-13.39	
23	88.37238	-10.3046	J055329.37-101816.4	9.27	8.65	8.55	8.43	8.47	8.4	8.41	Class III	-	1.29	0.19	9.20	-13.57	
24	88.34882	-10.2910	J055323.71-101727.4	16.8	15.8	14.0	11.6	9.74	7.78	5.57	Protostar	-	0.84	0.16	7.70	-13.76	
25	88.43061	-10.1900	J055343.34-101124.0	14.3	13.6	13.3	13.1	13	12.0	8.34	Class III	-	1.11	0.30	4.60	-13.64	
26	88.34597	-10.2923	J055323.03-101732.2	17.3	16.3	14.3	12.4	9.97	7.32	3.68	Protostars	-	< 0.84	-	-	< -13.76	
27	88.38743	-10.4534	J055332.98-102712.2	15.7	13.6	12.4	11.2	10.4	8.35	5.59	Class II	7	< 0.45	-	-	< -14.03	
28	88.29652	-10.5440	J055311.16-103238.3	10.7	10.3	10.1	9.89	9.7	8.43	6.6	Trans. Disk	-	< 7.09	-	-	< -12.83	
29	88.35579	-10.4543	J055325.39-102715.6	13.9	12.4	11.7	11.1	10.4	8.51	6.12	Class II	5	< 0.46	-	-	< -14.02	Tentative
30	88.44192	-10.5811	J055346.06-103452.1	13.7	12.7	12.1	11.2	10.6	8.26	6.19	Class II	-	< 1.04	-	-	< -13.67	
31	88.35442	-10.4584	J055325.06-102730.1	13.1	11.8	11	10.1	9.35	6.92	4.8	Class II	4	< 0.48	-	-	< -14.00	